Neoplasia 47 (2024) 100952

Contents lists available at ScienceDirect

Neoplasia

journal homepage: www.elsevier.com/locate/neo

Original Research

Secreted insulin-like growth factor binding protein 5 functions as a tumor suppressor and chemosensitizer through inhibiting insulin-like growth factor 1 receptor/protein kinase B pathway in acute myeloid leukemia

Beiying Zhang [a,b], Xiaoling Deng [c,d], Ruolan You [a], Jingru Liu [a], Diyu Hou [a], Xiaoting Wang [a], Shucheng Chen [a], Dongliang Li [e], Qiang Fu [f], Jingdong Zhang [c], Huifang Huang [a,**], Xiaoli Chen [c,d,*]

[a] Central Laboratory, Fujian Medical University Union Hospital, 29 Xinquan Road, Fuzhou, Fujian 350001, China
[b] Department of Laboratory Medicine, The First Hospital of Quanzhou Affiliated to Fujian Medical University, Quanzhou, Fujian 362000, China
[c] Jiangxi Health Commission Key Laboratory of Leukemia, the Affiliated Ganzhou Hospital of Nanchang University, No 16 Meiguan Road, Ganzhou, Jiangxi 341000, China
[d] Ganzhou Key Laboratory of Molecular Medicine, the Affiliated Ganzhou Hospital of Nanchang University, Ganzhou, Jiangxi 341000, China
[e] Department of Hepatobiliary Disease, the 900th Hospital of the People's Liberation Army Joint Service Support Force, Fuzhou, Fujian 350025, China
[f] Fujian Institute of Hematology, Fujian Provincial Key Laboratory on Hematology, Fujian Medical University Union Hospital, Fuzhou, Fujian 350001, China

ARTICLE INFO

Keywords:
Acute myeloid leukemia
IGFBP5
Tumor suppressor
Chemosensitizer
Subcellular localization

ABSTRACT

Background: In addition to being secreted into the intercellular spaces by exocytosis, insulin-like growth factor binding protein 5 (IGFBP5) may also remain in the cytosol or be transported to the nucleus. Depending on the different cellular context and subcellular distribution, IGFBP5 can act as a tumor suppressor or promoter through insulin-like growth factor -dependent or -independent mechanisms. Yet, little is known about the impacts of IGFBP5 on acute myeloid leukemia (AML) and its underlying mechanism.

Methods: Here we investigated the roles of IGFBP5 in human AML by using recombinant human IGFBP5 (rhIGFBP5) protein and U937 and THP1 cell lines which stably and ectopically expressed IGFBP5 or mutant IGFBP5 (mtIGFBP5) with the lack of secretory signal peptide. Cell counting kit-8 and flow cytometry assay were conducted to assess the cell viability, cell apoptosis and cell cycle distribution. Cytotoxicity assay was used to detect the chemosensitivity. Leukemia xenograft model and hematoxylin-eosin staining were performed to evaluate AML progression and extramedullary infiltration *in vivo*.

Results: In silico analysis demonstrated a positive association between *IGFBP5* expression and overall survival of the AML patients. Both *IGFBP5* overexpression and extrinsic rhIGFBP5 suppressed the growth of THP1 and U937 cells by inducing cell apoptosis and arresting G1/S transition and promoted the chemosensitivity of U937 and THP1 cells to daunorubicin and cytarabine. However, overexpression of *mtIGFBP5* failed to demonstrate these properties. An *in vivo* xenograft mouse model of U937 cells also indicated that overexpression of *IGFBP5* rather than *mtIGFBP5* alleviated AML progression and extramedullary infiltration. Mechanistically, these biological consequences depended on the inactivation of insulin-like growth factor 1 receptor -mediated phosphatidylinositol-3-kinase/protein kinase B pathway.

Abbreviations: AML, acute myeloid leukemia; IGFBP5, insulin-like growth factor binding protein 5; rhIGFBP5, recombinant human IGFBP5; mtIGFBP5, mutant form of IGFBP5 with deletion of N-terminus secretory signal peptide; IGFs, insulin-like growth factors; IGF1R, insulin-like growth factor 1 receptor; AKT, protein kinase B; PI3K, phosphatidylinositol-3-kinase; CDS, coding sequence; IC50, the half maximal inhibitory concentration; APC, allophycocyanin; 7-AAD, 7-amino-actinomycin; CCKc, cell counting kit; FBS, fetal bovine serum; RT-qPCR, real time quantitative polymerase chain reaction; Ara-C, cytarabine; DNR, daunorubicin; PI, propidium iodide; OS, overall survival; CST, cell signaling technology; PTEN, phosphatase and tensin homolog deleted on chromosome ten; GAPDH, glyceraldehyde 3-phosphate dehydrogenase; CDK, cyclin-dependent kinase; mRNA, message RNA; ELISA, enzyme-linked immunosorbent assay; OE, overexpression; NCG, NOD-Prkdc^{em26Cd52}il2rg^{em26Cd22}/Nju; ANOVA, analysis of variance.

* Corresponding author at: Jiangxi Health Commission Key Laboratory of Leukemia, the Affiliated Ganzhou Hospital of Nanchang University, No 16 Meiguan Road, Ganzhou, Jiangxi 341000, China.
** Corresponding author.
E-mail addresses: huanghuif@fjmu.edu.cn (H. Huang), fsgzyy2805@ncu.edu.cn (X. Chen).

https://doi.org/10.1016/j.neo.2023.100952
Received 27 September 2023; Received in revised form 3 December 2023; Accepted 11 December 2023
Available online 29 December 2023

Conclusions: Our findings revealed secreted rather than intracellular IGFBP5 as a tumor-suppressor and chemosensitizer in AML. Upregulation of serum IGFBP5 by overexpression or addition of extrinsic rhIGFBP5 may serve as a suitable therapeutic approach for AML.

Introduction

As a group of heterogeneous hematopoietic malignancies, acute myeloid leukemia (AML) is characterized with the excessive growth of immature myeloid blasts and the arrested myeloid differentiation in bone marrow [1]. In adults, it makes up 80 % of acute leukemia cases [2]. Even with continuous treatment, majority of the patients still suffer from the relapse within 5 years and ultimately succumb to this disease [3]. To effectively eradicate AML, new molecular-targeted therapies need to be developed.

Insulin-like growth factors (IGFs) system mainly consists of two polypeptide hormones (IGF1 and IGF2), two surface receptors (IGF1R and IGF2R), and six IGF-binding proteins (IGFBP1-6) [4]. Besides regulating cell/tissue development, this signaling axis also plays a pivotal role in malignant cell transformation [5]. IGF1R mediates most actions of IGF1 and IGF2 through its tyrosine kinase activity [6]. As flexible autocrine, paracrine, or endocrine proteins, IGF-binding proteins (IGFBPs) may suppress IGFs actions by blocking their binding to IGF1R, but they may also potentiate IGFs actions by serving as a reservoir for IGFs [7]. Furthermore, intracellular IGFBPs have IGFs-independent actions, such as regulation of intranuclear transcription [8].

As the most conserved member of IGFBPs family, insulin-like growth factor binding protein 5 (IGFBP5) was originally identified as a secretory protein which binds with high affinity to IGFs through its N-terminal domain and exerted its anti-apoptotic and mitogenic effects [9]. The diverse biological functions of IGFBP5 vary depending on its subcellular localization. Upon translocation into the nucleus, it may act as a transcription activator [10]. IGFBP5 suppresses or accelerates tumor growth through IGF/IGF1R-dependent or -independent mechanisms [11]. Different cellular contexts may account for these contradictory effects [12]. It had been reported that autocrine IGF1 promoted AML cell proliferation *via* the IGF1R/phosphatidylinositol-3-kinase (PI3K)/ protein kinase B (AKT) pathway [13]. As a kinase inhibitor of IGF1R, NVP-ADW742 hampered AML cell survival and enhanced their chemosensitivity to cytarabine (Ara-C) [14]. However, the effect of IGFBP5 on AML pathogenesis is not well defined.

To better comprehend the roles of IGFBP5 in AML, we focus on the following aspects in our current research: (1) to investigate the exact effects of IGFBP5 on AML; (2) to determine whether secreted or intracellular IGFBP5 is responsible for AML progression; and (3) to explore the signaling pathways regulated by IGFBP5. Here we performed *in silico* analysis of three databases and found a strong positive relationship between *IGFBP5* expression and overall survival (OS) of the AML patients. We further identified secreted rather than intracellular IGFBP5 as a tumor suppressor and chemosensitizer by using the *IGFBP5/mtIGFBP5* (Mutant form of *IGFBP5* which lacked N-terminus secretory signal peptide) -transduced THP1 and U937 cells and the recombinant human IGFBP5 (rhIGFBP5) protein both *in vitro* and *in vivo*. Our findings demonstrated that secreted IGFBP5 may represent a novel therapeutic target, upregulation of which will contribute to retarding AML progression and enhancing the chemosensitivity of AML cells to Ara-C and daunorubicin (DNR).

Materials and methods

Survival analysis

To assess the prognostic significance of IGFBP5 in AML, we compared the OS rates between the AML patients with elevated *IGFBP5* expression and those with reduced *IGFBP5* expression using three publicly available databases: UALCAN (The University of Alabama at Birmingham Cancer data analysis portal) databases (http://ualcan.path.uab.Edu/analysis.Html; n = 163), TCGA (The Cancer Genome Atlas) portal databases (http://tumorsurvival.org/index.Html; n = 151), and GEPIA2 (Gene Expression Profiling Interactive Analysis 2) databases (http://gepia2.cancer-pku.cn; n = 106). The Kaplan-Meier curves were downloaded from the 'Survival Analysis' sections of their website.

Cell lines and culture condition

Except for NB4 cells from Prof. Xiaoming Feng (Institute of Hematology and Blood Diseases Hospital, Chinese Academy of Medical Sciences & Peking Union Medical College), other five human AML cell lines were purchased from the Cell Bank of Type Culture Collection of the Chinese Academy of Sciences (Shanghai, China). MV4-11, NB4, THP1 and U937 cells were cultured in Roswell Park Memorial Institute-1640 medium (Hyclone, Logan, UT, USA) supplemented with 10 % fetal bovine serum (FBS, Gemini Bio-Products, Sacramento, CA, USA), while HL-60 and KG1 cells were grown in Iscove's modified Dulbecco's medium (Hyclone, Logan, UT, USA) containing 20 % FBS. Human embryonic kidney (HEK)-293T cells were maintained in Dulbecco's modified Eagle's medium/high glucose (Hyclone, Logan, UT, USA) containing 10 % FBS, penicillin (100 U/mL) and streptomycin (100 μg/mL) (Invitrogen, Carlsbad, CA). All the cells were maintained in a humidified incubator at 37 °C with 5 % CO_2. U937 and THP1 cells were exposed with 500 ng/mL rhIGFBP5 protein (R&D System, Minneapolis, MN, USA) for 5 days to conduct the proliferation inhibition assay.

Pharmacological agents, plasmids and primers

A full-length coding sequence (CDS) fragment of human *IGFBP5* was obtained from HEK-293T cells by reverse transcriptase polymerase chain reaction and inserted into BamHI and EcoRI sites of lentiviral vector pCDH-CMV-MCS-EF1-copGFP-T2A-Puro (System Biosciences, SBI). To increase the translation efficiency, a Kozak consensus sequence ACC was embedded in front of the translation initiation site. *mtIGFBP5* was generated by PCR-mediated deletion using human *IGFBP5* CDS as templates and cloned into the vector described above. The primers for PCR assay were obtained from Sangon Biotech Co., Ltd (Shanghai, China). Details of the primer sequences are shown in Table 1. DNR (Shandong New Era Pharmaceutical Co. Ltd, Linyi, China) and Ara-C (Pharmacia, Italy) were purchased from the Central Pharmacy of Fujian Medical University Union Hospital (Fuzhou, China).

Table 1
Primer sequences for candidate genes.

Gene	Sequence (5′-3′)
Human IGFBP5 CDS Forward Primer	CGGAATTCACCATGGTGTTGCTCACCGCGGTC
Human IGFBP5 CDS Reverse Primer	CGGGATCCTCACTCAACGTTGCTGCTGTC
Human mtIGFBP5 Forward Primer	CGGAATTCACCATGCTGGGCTCCTTCGTGCACTG
Human IGFBP5 Forward Primer	ACCTGAGATGAGACAGGAGTC
Human IGFBP5 Reverse Primer	GTAGAATCCTTTGCGGTCACAA
Human β-actin Forward Primer	CCACGAAACTACCTTCAACTCC
Human β-actin Reverse Primer	GTGATCTCCTTCTGCATCCTGT

Lentivirus production and cell infection

For lentivirus packaging, the expression vector was co-transfected with the packaging plasmid psPAX2 (Addgene) and the envelope plasmid pMD2.G (Addgene) into HEK-293T cells at a ratio of 4:3:1 using lipofector 3000 (Promega, Madison, WI, USA). Viral supernatants were collected at 48 and 72 h after transfection. U937 and THP1 cells were infected with the viral supernatants supplemented with 4 μg/mL polybrene (Sigma-Aldrich, USA) *via* centrifugation for 2 h at 37 °C at 800 g. Infected cells were selected for more than 7 days with puromycin (2.5 μg/mL) (Sigma-Aldrich, USA). The untreated parental cells and those transduced with the empty vector were served as the blank and the control, respectively.

Cell counting kit-8 (CCK-8) assay

U937 and THP1 cells (20 000 cells per well) in the logarithmic growth phase were placed into 96-well plates and incubated in a humidified incubator with 5 % CO_2 at 37 °C for 1, 2, 3, 4 or 5 days. The cells were cultured for another 2 h after being filled with 10 μL CCK-8 (Dojindo Molecular Technologies, Japan) and the absorbance at 450/630 nm were measured with a microplate reader (Thermo Fisher Scientific).

Cytotoxicity assay

Cytotoxicity assay was conducted to assess the chemosensitivity of AML cells to DNR and Ara-C. U937 and THP1 cells in the logarithmic growth phase were seeded into 96-well plates at 20 000 cells per well and treated with DNR or Ara-C at indicated concentrations for 24 h. Then the cell viabilities were detected using CCK-8 assay according to the manufacturer's instruction. The corrected absorbance values were used to calculate the half-maximal inhibitory concentration (IC50) values with GraphPad Prism.

Apoptosis assay

Cell apoptosis was detected with Annexin V-allophycocyanin (APC) Apoptosis Detection Kit (KeyGEN BioTECH, Jiangsu, China). The cells were collected, washed and resuspended in 100 μL Annexin V binding buffer to a final concentration of 10^6 cells per mL and incubated with 5 μL 7-aminoactinomycin (7-AAD) and 5 μL Annexin V-APC solution for 15 min at room temperature in the dark. Finally, the cells were resuspended in 400 μL of Annexin V binding buffer and immediately analyzed with a FACSCalibur flow cytometer (Becton Dickinson). FlowJo software (TreeStar) was used for data analysis.

Cell cycle assay

Cell cycle distributions of U937 and THP1 cells were detected with propidium iodide (PI) staining and flow cytometry. U937 or THP1 cells were harvested and washed with phosphate-buffered saline (Dingguochangsheng, Beijing, China), and then fixed for 12 h at -20 °C in 70 % ethanol. Cells were incubated with RNase A (100 μg/mL, Thermo Fisher Scientific) and PI (10 μg/mL, BD Pharmingen) for 30 min at 37 °C in the dark. The stained samples were immediately analyzed with a flow cytometer. The data analyses were conducted using FlowJo software.

Western blot

The cells were lysed in radio-immunoprecipitation assay lysis buffer containing protease and phosphatase inhibitor cocktail (Sigma-Aldrich). The bicinchoninic acid Protein Assay Kit (Thermo Fisher Scientific, Carlsbad, CA, USA) was used to quantify protein concentration. Total proteins (25-40 μg /lane) were separated by 8-12 % sodium dodecyl sulfate-polyacrylamide gel electrophoresis and then transferred to polyvinylidene fluoride membranes (Millipore, USA). The membranes were probed for overnight at 4°C with the appropriate primary antibody and then incubated for 2 h at room temperature with horseradish peroxidase-conjugated secondary antibody (Cat No.7074; Cell Signaling Technology (CST)). The signals were detected using the chemiluminescence SuperSignal kit (Pierce). The primary antibodies used were as follows: IGFBP5 (Cat No. 10941; CST), IGF1R (Cat No. 9750; CST), phosphorylated (p)-IGF1R β/Irβ (Tyr1131/ Tyr1146) (Cat No. 80732; CST), phosphatase and tensin homolog deleted on chromosome ten (PTEN, Cat No. 9188; CST), PI3K (Cat No. 4257; CST), p-PI3K (Tyr458) (Cat No. 17366; CST), AKT (Cat No. 9272; CST), p-AKT (Ser473) (Cat No. 4060; CST), glyceraldehyde 3-phosphate dehydrogenase (GAPDH, AF0006; Beyotime), p21 (Cat No. 2847; CST), cyclin-dependent kinase 2 (CDK2, Cat No. 18048; CST), cyclin-dependent kinase 4 (CDK4, Cat No. 12790; CST), cyclin-dependent kinase 6 (CDK6, Cat No. 13331; CST), Cyclin D1 (Cat No. 55506; CST), Cyclin E1 (Cat No. 20808; CST), β-actin (AA128; Beyotime).

Real-time quantitative PCR (RT-qPCR)

The RNA transcripts of interest genes were determined by RT-qPCR. Total RNA was extracted from cells using TRIzol reagent (Invitrogen, ThermoFisher Scientific) according to the manufacturer's protocol. Avian myeloblastosis virus reverse transcriptase (Takara, Japan) was used to reverse-transcribe message RNA (mRNA) into complementary DNA from 1 μg total RNA. RT-qPCR was conducted in triplicate 20 μL reactions (250 nM each primer, 10 μL Master Mix) following the manufacturer's instruction (Roche Applied Science, Basel, Switzer). The relative mRNA levels of target genes were normalized to β-actin.

Enzyme-linked immunosorbent assay (ELISA)

ELISA was conducted to quantify the concentrations of IGFBP5 protein in the culture supernatants. The culture supernatants were harvested after a 72 h incubation and centrifuged at 13,000 rotations per minute for 10 min to remove cell debris. IGFBP5 protein levels were measured using commercially available human IGFBP5 ELISA Kit (CSB-E13263h, CUSABIO, China) following the manufacturer's instructions.

AML cells xenograft models

The animal experiments were conducted with wild type six-week-old female NOD-Prkdc^{em26Cd52}il2rg^{em26Cd22}/Nju (NCG) mice (Model Animal Research Center of Nanjing University) according to the experiment protocol approved by the Institutional Animal Care and User Ethics Committee of Fujian Medical University/Laboratory Animal Center (Fuzhou, China) (No. FJMUIACUC2021-0352). The mice were kept in a specific pathogen-free facility at 22C under a 12 h light/dark cycle with access to water and food *ad libitum*. U937 cells (4.0×10^5 cells per mouse) were transplanted into NCG mice by tail vein injection. The recipient mice were randomly assigned into three groups basing on the transplanted cells, including control (U937 cells carrying empty vector), IGFBP5-OE (IGFBP5 overexpression, U937 cells carrying IGFBP5), mtIGFBP5-OE (mtIGFBP5 overexpression, U937 cells carrying mtIGFBP5). Mice were closely monitored for disease manifestation and sacrificed when any mice began to show the signs of leukemic terminal illness (such as coma, prostration). The proportions of the transplanted cells in liver, spleen and bone marrow were detected with an APC-labeled antibody to human CD45 (BD-Biosciences, NJ, USA) by Flow Cytometer. Extramedullary invasion was evaluated using histochemical analysis. The harvested liver and spleen were fixed in 4 % paraformaldehyde for more than 24 h, embedded in paraffin, serially sectioned into 5 μm-thick slices, stained with hematoxylin-eosin, and photographed.

Statistical analysis

The statistical analyses were conducted with GraphPad prism 5.0 and SPSS 19.0 software. Data were presented as mean ± standard deviation. Kaplan-Meier curve was used to analyze the survival distribution of the two groups. Shapiro-Wilk test and Levene's test were conducted to verify the distribution's normality and homogeneity of variance respectively. For the data with normal distribution and homogeneity of variance, a two-tailed Student's t-test was used to determine the statistical distinctions between two groups, while a one-way analysis of variance (ANOVA) test with Tukey's test was employed for conducting multiple group comparisons. For the non-normally distributed data or data without homogeneity of variance, Mann-Whitney U tests and Kruskal-Wallis followed by Dunn's multiple comparison tests were used for two group comparisons and multiple group comparisons respectively. Statistical significances were indicated as $*P < 0.05$, $**P < 0.01$, $***P < 0.001$ and ns, not significant.

Results

IGFBP5 expression was positively correlated with OS of the AML patients

To assess the prognostic value of *IGFBP5* expression in AML, *in silico* analyses were conducted to determine the potential correlation between *IGFBP5* expression and OS of the AML patients using the data from three independent databases. The results showed that there was a better OS for AML patients with high IGFBP5 expression than those with low IGFBP5 expression ($P = 0.05$ in UALCAN; $P = 0.0083$ in TCGA; $P = 0.087$ in GEPIA2) (Fig. 1A–C). The expression levels of *IGFBP5* among AML French-American-British subtypes were determined using the data from the UALCAN databases. We found that *IGFBP5* expression was relatively lower in the M5 subtype compared with other AML subtypes (Fig. 1D). RT-qPCR was performed to detect the expression levels of *IGFBP5* in different AML cell lines. Concordantly, THP1 and U937 cells which were considered as human AML-M5 cells displayed the relative lower expression of *IGFBP5* compared with other AML cell lines ($P < 0.05$; Fig. 1E).

Overexpression of IGFBP5 inhibited AML cell proliferation and increased the chemosensitivity of AML cells to DNR and Ara-C

We employed a gain-of-function approach to test the function of IGFBP5 on AML. THP1 and U937 cells which lowly expressed endogenous IGFBP5 were selected to ectopically express IGFBP5 using a lentivirus system. Overexpression of *IGFBP5* in IGFBP5-tranduced U937 and THP1 cells were verified by RT-qPCR assay and western blot assay (Fig. 2A, B). Using these cell lines, we first performed an *in vitro* cell proliferation experiment with CCK-8 assay and observed significant

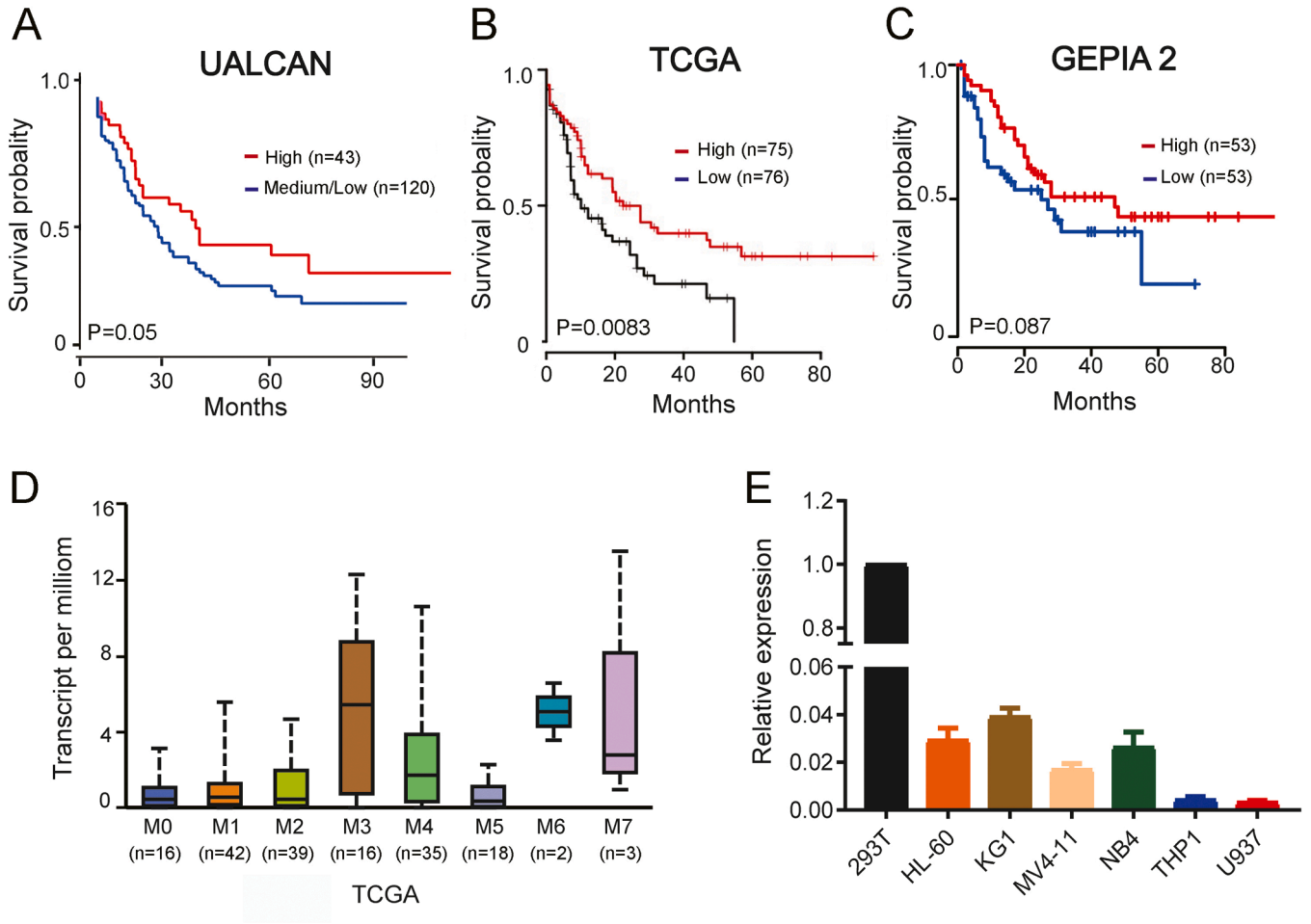

Fig. 1. IGFBP5 expression is positively correlated with overall survival of the AML patients.
(A-C) IGFBP5 expression is positively correlated with overall survival of the AML patients (left, UALCAN, p = 0.05; middle, TCGA, P= 0.0083; right, GEPIA2, p = 0.087). Patients were divided into two groups based on whether IGFBP5 expression was high or medium/low (A) and high or low (B, C) according to the ranking of expression levels. Survival vs time is plotted. Kaplan-Meier curve was used to analyze the survival distribution of the two groups. (D) *In silico* analysis of human IGFBP5 mRNA expression in different AML subtypes based on the data from the UALCAN databases (n=195). (E) RT-qPCR analysis of IGFBP5 mRNA expression in AML cell lines (n=3).

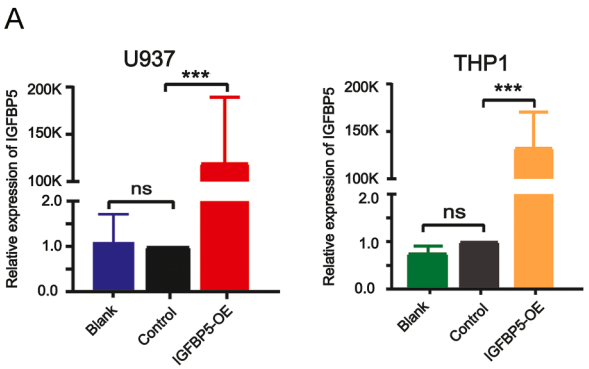

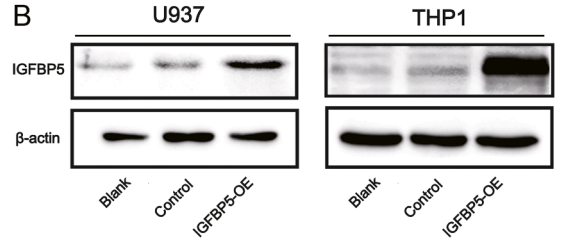

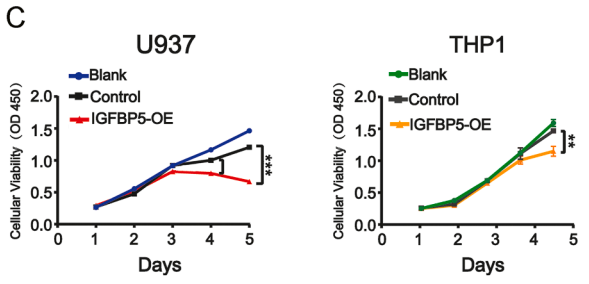

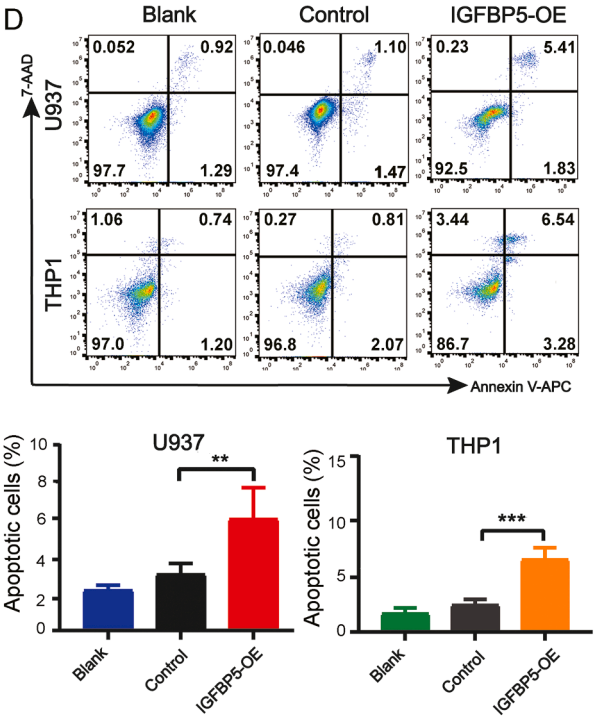

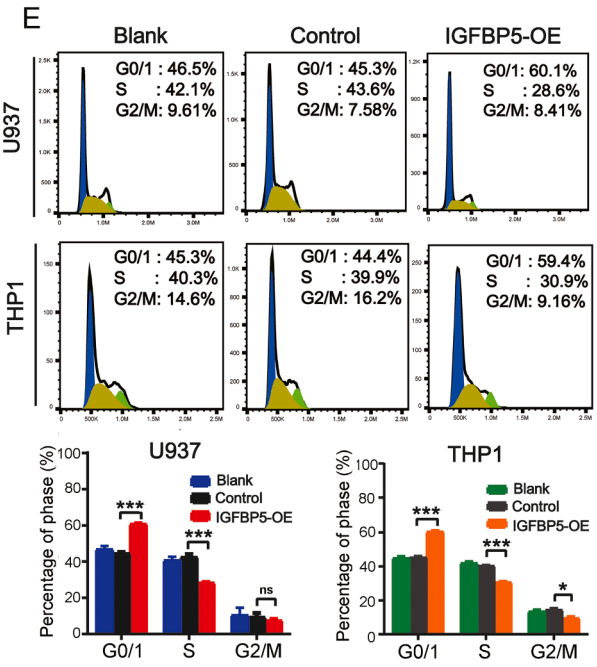

F

	U937 +Ara-C	U937+DNR	THP1 +Ara-C	THP1+ DNR
Blank/IC50 (μM)	0.931±0.075	0.297±0.034	5.536±0.202	0.310±0.023
Control/IC50 (μM)	0.911±0.036	0.267±0.069	5.282±0.595	0.283±0.053
IGFBP5-OE/IC50 (μM)	0.620±0.021	0.152±0.017	3.126±0.559	0.175±0.012
mtIGFBP5-OE/IC50 (μM)	0.884±0.047	0.260±0.009	5.167±0.071	0.260±0.048
P value	1.>0.05	1.>0.05	1.>0.05	1.>0.05
	2.<0.05	2.<0.05	2.<0.05	2.<0.05
	3.>0.05	3.>0.05	3.>0.05	3.>0.05

1.Blank *VS* Control; 2. IGFBP5-OE *VS* Control; 3. mtIGFBP5-OE *VS* Control

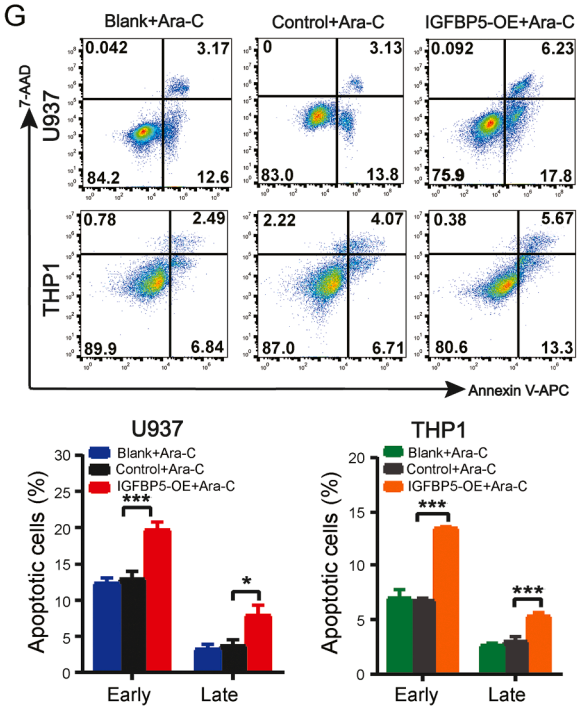

(caption on next page)

Fig. 2. IGFBP5 overexpression significantly suppresses AML cells proliferation.
(A) RT-qPCR validation of the upregulated expression of IGFBP5 in the IGFBP5-transduced U937 and THP1 cells (n=3). (B) Immunoblotting validation of the upregulated expression of IGFBP5 in the IGFBP5-transduced U937 and THP1 cells. β-actin was used as a loading control. (C) Growth inhibitory effects of the ectopically expressed IGFBP5 on U937 and THP1 cells. Cell viability was measured by CCK-8 assay at the indicated time points (day 1, day 2, day 3, day 4, day 5) (n=3). (D) Overexpression of IGFBP5 can induce cell apoptosis in U937 and THP1 cells. The percentages of apoptotic cells were determined by flow cytometry using Annexin V/7-AAD staining. Shown are representative flow plots. The quantification is shown at the bottom. (E) Overexpression of IGFBP5 can induce cell cycle arrest at G0/G1 phase in U937 and THP1 cells. Cells were stained with PI and analyzed by flow cytometry. Shown are representative flow plots. The quantification is shown at the bottom. (F) Secreted rather than intracellular IGFBP5 can sensitize U937 and THP1 cells to DNR and Ara-C. Growth inhibition of AML cells was tested by CCK-8 assay after treatment with different concentrations of DNR or Ara-C for 24 h. The IC50 values were determined according to dose–response curves using GraphPad Prism 5.0 software. Data are expressed as mean ± standard deviation. (G) Overexpression of IGFBP5 enhances Ara-C-induced cell apoptosis in U937 and THP1 cells. U937 and THP1 cells were treated with 0.5 μM and 2 μM Ara-C for 24 h respectively and then apoptotic cells were detected by flow cytometry using Annexin V/7-AAD staining. Shown are representative flow cytometry plots. The quantification is shown at the bottom. Blank: the untreated parental cells; Control: the empty vector -transduced cells; IGFBP5-OE: the IGFBP5-transduced cells. Statistical significance was determined by ANOVA with Tukey's multiple comparison test. * $P < 0.05$; ** $P < 0.01$; *** $P < 0.001$; ns, not significant.

proliferation inhibitions in the IGFBP5-transduced U937 and THP1 cells (IGFBP5-OE) at day 5 compared with those cells transduced with empty vector (Control) ($P < 0.001$ for U937; $P < 0.01$ for THP1) (Fig. 2C). We next addressed the roles of IGFBP5 in apoptosis and cell cycle arrest. The cells were stained with 7-AAD and Annexin V-APC to assess apoptosis. Overexpression of *IGFBP5* resulted in remarkable increases (~ 3-fold) of apoptotic cells compared with the empty vector control ($P < 0.01$ for U937; $P < 0.001$ for THP1) (Fig. 2D). The IGFBP5-transduced cells also displayed remarkable increases in G0/G1 phase fraction ($P < 0.001$ for both U937 and THP1) and decreases in S-phase fraction ($P < 0.001$ for both U937 and THP1) compared with the empty vector control (Fig. 2E).

To explore whether IGFBP5 can sensitize AML cells to chemotherapy-induced cell death. Cytotoxicity tests were performed with the indicated concentrations of drugs to determine the IC50 values at 24 h. The results demonstrated that the IGFBP5-transduced cells were more sensitive to Ara-C (0.620 ± 0.021 μM *vs* 0.911 ± 0.036 μM for U937, $P < 0.05$; 3.126 ± 0.559 μM *vs* 5.282 ± 0.595 μM for THP1, $P < 0.05$) and DNR (0.152 ± 0.017 μM *vs* 0.267 ± 0.069 μM for U937, $P < 0.05$; 0.175 ± 0.012 μM *vs* 0.283 ± 0.053 μM for THP1, $P < 0.05$) compared with the empty vector-transduced cells (Fig. 2F). The IGFBP5-transduced cells also demonstrated higher level of early and late cell apoptosis following exposure to Ara-C for 24 h. For example, after 24 h of exposure to 0.5 μM Ara-C, the IGFBP5-transduced U937 cells showed 17.8 % early apoptosis and 6.23 % late apoptosis, which were much higher than empty vector-transduced U937 cells (13.8 % and 3.13 %, respectively). After treatment with 2 μM Ara-C for 24 h, the IGFBP5-transduced THP1 cells displayed 13.3 % early apoptosis and 5.67 % late apoptosis, while the empty vector-transduced THP1 cells demonstrated lower levels of apoptosis, with only 6.71 % of cells in early apoptosis, 4.07 % of cells in late apoptosis (Fig. 2G).

Overexpression of IGFBP5 inhibited IGF1R activity by exocytosis in AML cells

To determine whether the observed growth inhibitions of the IGFBP5-transduced cells were due to the secreted IGFBP5, we quantified the concentrations of IGFBP5 protein in the culture supernatants by ELISA assay to verify IGFBP5 exocytosis. The result shows that *IGFBP5* overexpression in U937 and THP1 cells led to 30-fold higher concentrations in the culture supernatants. IGFBP5 levels in the culture supernatants of IGFBP5- transduced U937 and THP1 cells were 301.40 ± 3.99 ng/mL and 298.00 ± 4.96 ng/mL, respectively, which were much higher than those of the empty vector-transduced cells (9.70 ± 0.46 ng/mL for U937, 6.31 ± 0.49 ng/mL for THP1) ($P < 0.001$ for U937; $P < 0.001$ for THP1) (Fig. 3A). To further confirm whether secreted IGFBP5 regulates IGF1R activity, we detected the phosphorylation of IGF1Rβ (Tyr1131) by western blot and found that the phosphorylation of IGF1Rβ decreased upon IGFBP5 overexpression (Fig. 3B).

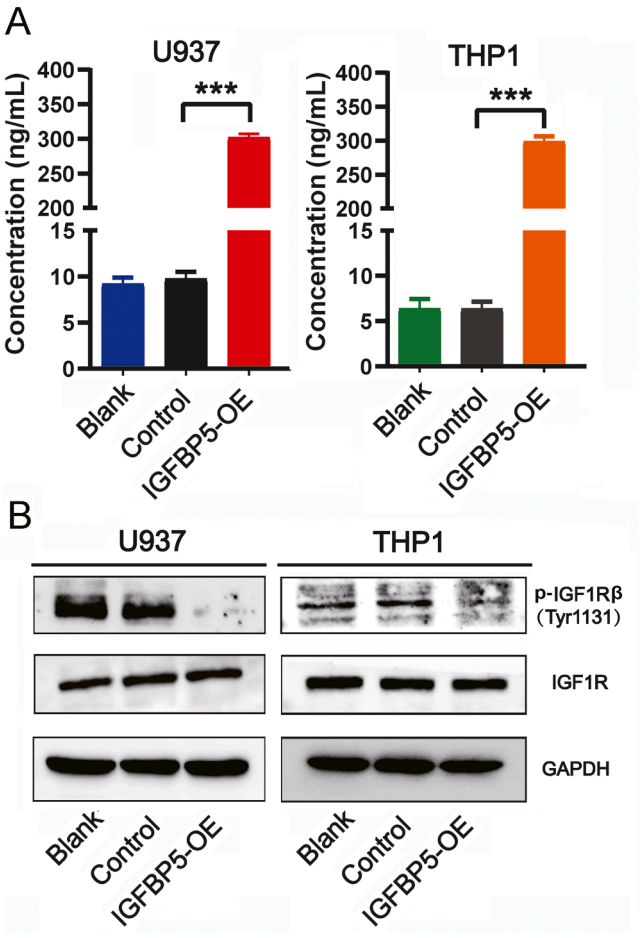

Fig. 3. IGFBP5 overexpression in AML cells inhibits IGF1R activity by secreting IGFBP5.
(A) ELISA qualification of IGFBP5 concentrations in the culture supernatants of IGFBP5-transduced U937 and THP1 cells. (B) Immunoblotting of p-IGF1R and total IGF1R protein in IGFBP5-transduced U937 and THP1 cells. GAPDH was used as a loading control. Blank: the untreated parental cells; Control: the empty vector -transduced cells; IGFBP5-OE: the IGFBP5 -transduced cells. Statistical significance was determined by ANOVA with Tukey's multiple comparison test. * P < 0.05; ** P < 0.01; *** P < 0.001; ns, not significant.

Extrinsic rhIGFBP5 also inhibited AML cell proliferation

We further assessed the impacts of extrinsic rhIGFBP5 protein on AML cell proliferation by Ki-67 staining coupled with flow cytometry. Cell proliferation was quantified by percentage of Ki-67$^+$ cells. Treatment with rhIGFBP5 led to a loss of Ki-67$^+$ viable cells ($P < 0.05$ for U937; $P < 0.01$ for THP1). The percentages of Ki-67$^+$ cells in untreated

U937 and THP1 cells were approximately 93.4 % and 97.9 %, respectively, but decreased to approximately 84.5 % and 75.9 % respectively after treatment with 500 ng/mL rhIGFBP5 protein for 72 h (Fig. 4A). Simultaneously, we detected cell apoptosis after treatment with 500 ng/mL rhIGFBP5 for 72 h and observed a remarkable increase in the percentages of early and late apoptotic cells (10.4 % early apoptosis and 5.35 % late apoptosis for U937 cells; 9.62 % early apoptosis and 5.89 % late apoptosis for THP1 cells) compared to the control cells (without rhIGFBP5 exposure) (both $P < 0.001$). The control cells showed very few apoptotic cells (1-2 %), which were considered as a background level of cell apoptosis (Fig. 4B). Cell cycle assay revealed that treatment with 500 ng/mL rhIGFBP5 protein for 72 h arrested the cell cycle at G1/S transition, which was exemplified by a notable increase in percentage of G1/G0 phase cells and a reduction in percentage of S phase cells (both $P < 0.05$) (Fig. 4C). Concordantly, rhIGFBP5 also inhibited IGF1R phosphorylation in U937 and THP1 cells (Fig. 4D).

Intracellular IGFBP5 had no effect on AML cell proliferation

We predicted the presence of 20 amino acids in the N-terminus of human IGFBP5 as a secretory signal peptide with SignaIP 4.0 server (http://www.cbs.dtu.dk/services/SignaIP/) (Fig. 5A). To exclude the interference of secreted IGFBP5, we constructed a Δ2-20 amino acid mtIGFBP5 which could escape from secretion. To determine whether intracellular IGFBP5 inhibits AML cell growth, we established the mtIGFBP5-transduced (mtIGFBP5-OE) U937 and THP1 cell lines by lentivirus system. We compared IGFBP5 protein levels in culture supernatants or whole-cell lysates between the mtIGFBP5-transduced cells and the empty vector control with ELISA and western blot assay. The results demonstrated no significant difference in culture supernatants (both $P > 0.05$) (Fig. 5B) but remarkable increases in the whole-cell lysates of the mtIGFBP5-transduced U937 and THP1 cells (Fig. 5C). Correspondingly, the ectopic mtIGFBP5 protein did not affect phosphorylation of IGF1Rβ (Fig. 5C). To assess mtIGFBP5's impacts on AML cell growth, we performed growth curve assay. No differences in cell growth rates were observed among the mtIGFBP5-transduced cells, the untreated blank cells, and the empty vector-transduced control cells (All $P > 0.05$; Fig. 5D). Furthermore, with these cells, we conducted cytotoxicity assay to measure IC50 values of Ara-C and DNR and no significant differences were observed among them (All $P > 0.05$; Fig. 2F).

Secreted IGFBP5 suppresses AML progression and extramedullary invasion in xenograft

By tail vein injection of U937 cells carrying IGFBP5, mtIGFBP5 or empty vector, we established a systemic xenogeneic AML model in

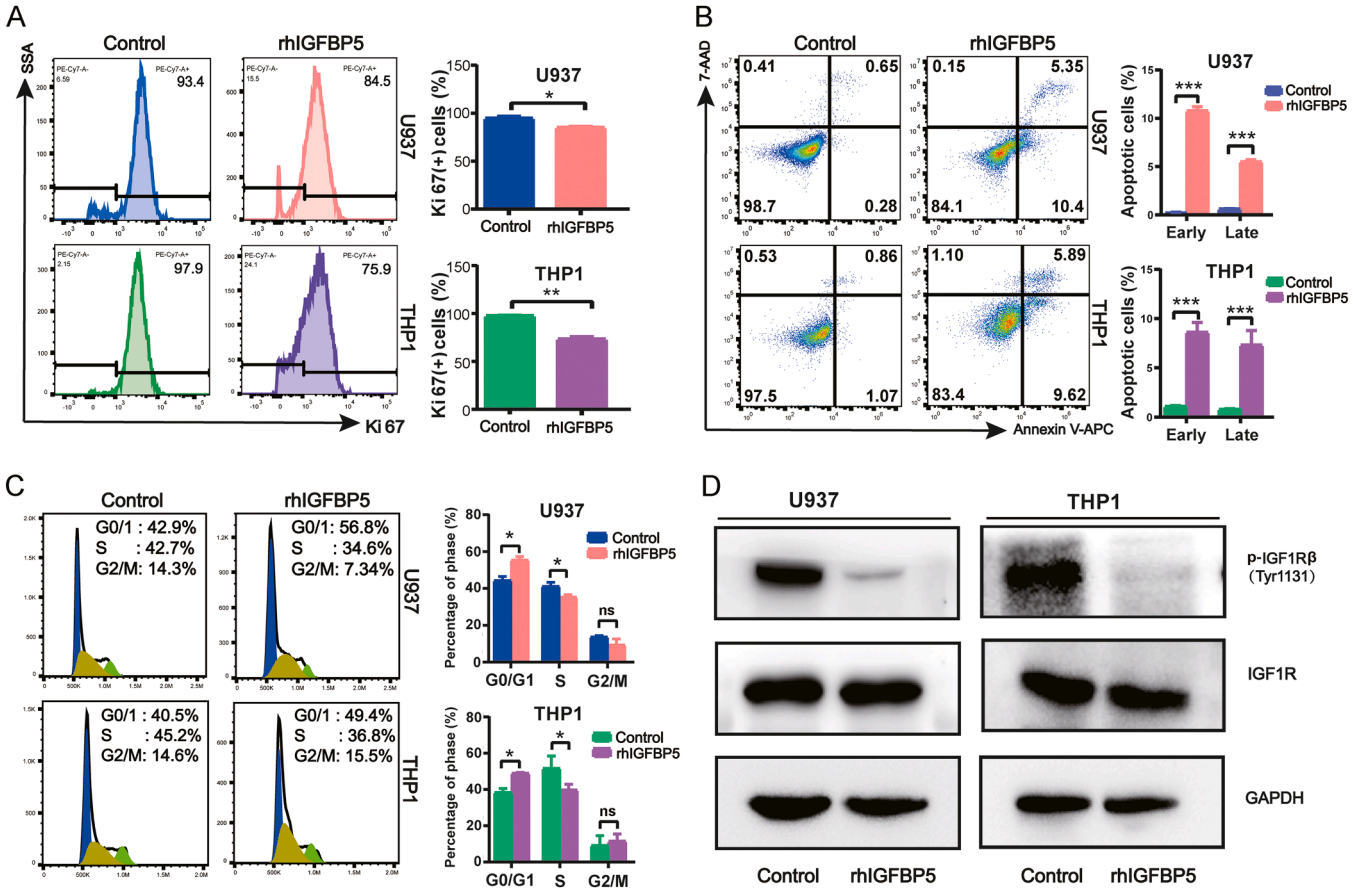

Fig. 4. Treatment with rhIGFBP5 suppresses AML cell proliferation.
(A) Representative flow plot of cell proliferation analysis by Ki-67 staining after rhIGFBP5 treatment (n=3). U937 or THP1 cells were treated with 500 ng/mL rhIGFBP5 protein for 72 h. The quantification is shown on the right. (B) Treatment with 500 ng/mL rhIGFBP5 protein induces cell apoptosis in U937 and THP1 cells. After treatment for 72 h, the cells were stained with 7-AAD and Annexin V-APC and analyzed by Flow Cytometry. Shown are representative flow cytometry plots. The quantification is shown on the right. (C) Treatment with 500 ng/mL rhIGFBP5 protein blocks G1-S phase transition in U937 and THP1 cells. After treatment for 72 h, the cells were stained with PI and analyzed by Flow Cytometry. Shown are representative Flow Cytometry plots. The quantification is shown on the right. (D) Immunoblotting of p-IGF1R and total IGF1R protein in U937 and THP1 cells after treatment with 500 ng/mL rhIGFBP5 for 72 h. GAPDH was used as a loading control. Control: the untreated cells; rhIGFBP5: the cells treated with 500 ng/mL rhIGFBP5 protein. Statistical significance was determined by unpaired Student's t test. * $P < 0.05$; ** $P < 0.01$; *** $P < 0.001$; ns, not significant.

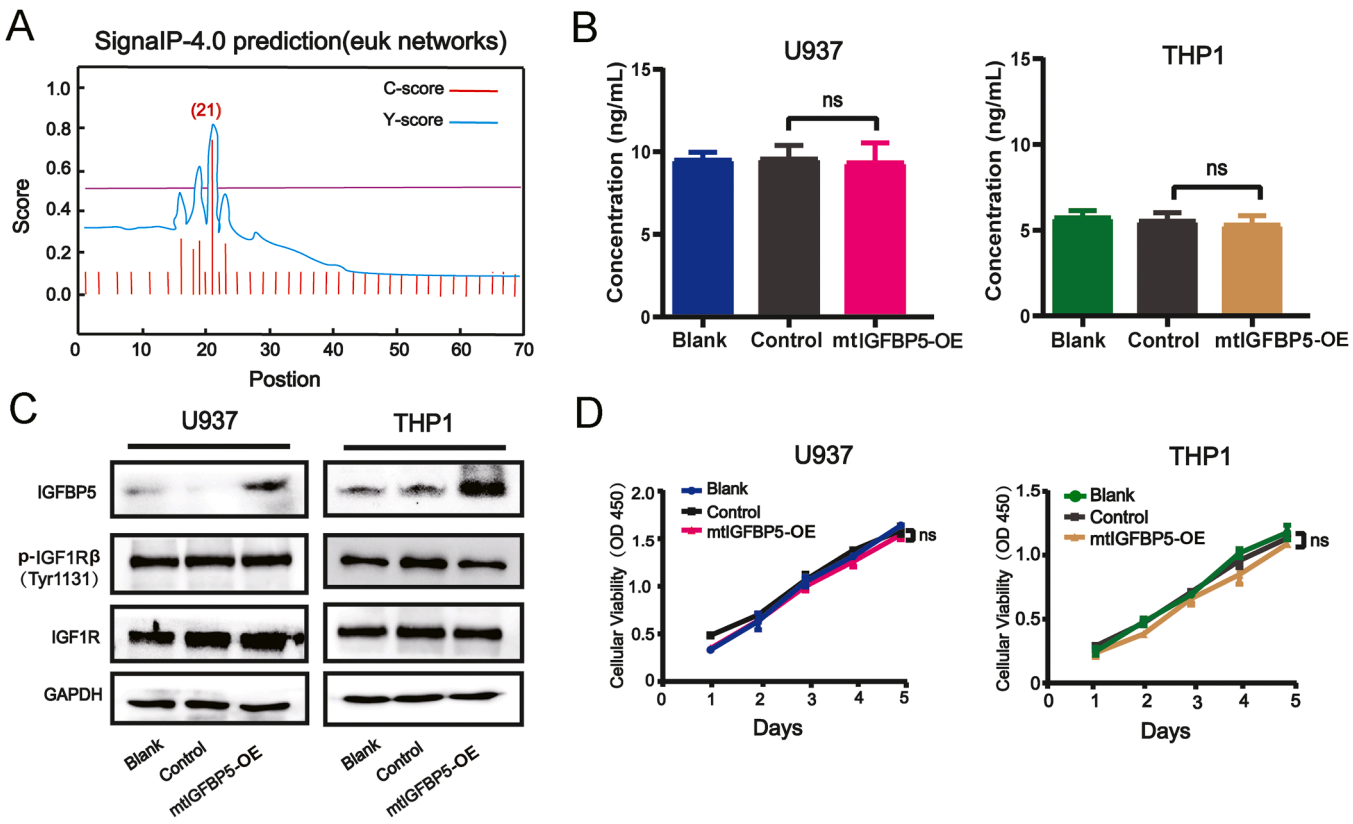

Fig. 5. Intracellular IGFBP5 has no effect on AML cell proliferation.
(A) Prediction of a secretory signal peptide containing 20 amino acid residues in N-terminus of IGFBP5 by SignaIP 4.0. (B) ELISA qualification of IGFBP5 concentrations in the culture supernatants of mtIGFBP5-transduced U937 and THP1 cells. (C) Immunoblotting of IGFBP5, p-IGF1R and total IGF1R protein in mtIGFBP5-transduced U937 and THP1 cells. GAPDH was used as a loading control. (D) The ectopical expression of mtIGFBP5 in U937 and THP1 cells has no effect on AML cell proliferation (n=3). Cell viability was measured by CCK-8 assay at the indicated time points (day 1, day 2, day 3, day 4, day 5). Blank: the untreated parental cells; Control: the empty vector-transduced cells; mtIGFBP5-OE: the mtIGFBP5-transduced cells. Statistical significance was determined by ANOVA with Tukey's multiple comparison test. * $P < 0.05$; ** $P < 0.01$; *** $P < 0.001$; ns, not significant.

immunodeficient NCG mice. As a result, all the recipients developed AML, but the mice transplanted with U937 cells carrying IGFBP5 (IGFBP5-OE) displayed lower proportions of engrafted AML cells (human CD45+ cells) in bone marrow, liver, and spleen compared with those transplanted with U937 cells carrying mtIGFBP5 (mtIGFBP5-OE) or empty vector (Control) at one month after transplantation (both $P < 0.001$) (Fig. 6A). The mice transplanted with U937 cells carrying IGFBP5 also exhibited significant decreases in size and weight of the liver and spleen (both $P < 0.001$) compared to those transplanted with U937 cells carrying mtIGFBP5 or empty vector (Fig. 6B). Histologically, the infiltrated leukemic cells in livers were particularly prominent around the portal veins and displayed smaller size, less cytosol, and irregular nuclei with clumped chromatin compared to hepatocytes. It was observed that the increased infiltrations of leukemic cell around the portal vein resulted in narrowing and blocking of vein in the mice transplanted with U937 cells carrying mtIGFBP5 or empty vector compared to those transplanted with U937 cells carrying IGFBP5. The infiltrated leukemic cells in spleen presented larger irregular nuclei with clumped chromatin compared to lymphocytes. *IGFBP5* overexpression led to much less infiltration of leukemic cells into spleen, which was embodied with less fading of germinal centers and red pulp and much less decrease in erythrocytes and lymphocytes (Fig. 6C). However, no significant difference was found between the mice transplanted with U937 cells carrying mtIGFBP5 and those transplanted with U937 cells carrying empty vector (Fig. 6A–C).

Secreted IGFBP5 exerts its effects via inhibiting IGF1R-mediated PTEN/PI3K/AKT pathway

To explore whether secreted IGFBP5 exerts its effects through the IGF1R-mediated PI3K/AKT pathway, we conducted western blot analyses to test the levels of several proteins related to this pathway, including PTEN, PI3K, AKT. The results demonstrated that the expression of p-PI3K, p-AKT were notably downregulated, but the expression of PTEN significantly increased in U937 and THP1 cells that stably overexpressed IGFBP5 (Fig. 7A). We detected the expression of some important cell cycle-related proteins by western blot and found that overexpression of *IGFBP5* in U937 and THP1 cells induced a striking upregulation of p21 protein and notably reductions of CDK2, CDK4, CDK8, Cyclin D1, and Cyclin E1 (Fig. 7B).

Discussion

IGFBP5's biological functions are not only determined by tissue and cell type but also depend on the cellular context, especially its interacting proteins and nuclear localization [6,15]. Here we found that the subcellular localization of IGFBP5 protein is crucial for its function in AML cells. We identified secreted rather than intracellular IGFBP5 as a novel suppressor and chemosensitizer in AML cells.

Several studies have reported conflicting results regarding the relationship between IGFBP5 expression and cancer patient survival. High levels of IGFBP5 predicted worse disease-free survival and OS in the patients with urothelial carcinomas [16], kidney renal papillary renal cell carcinoma [17] or colorectal cancer [18] but better recurrence-free

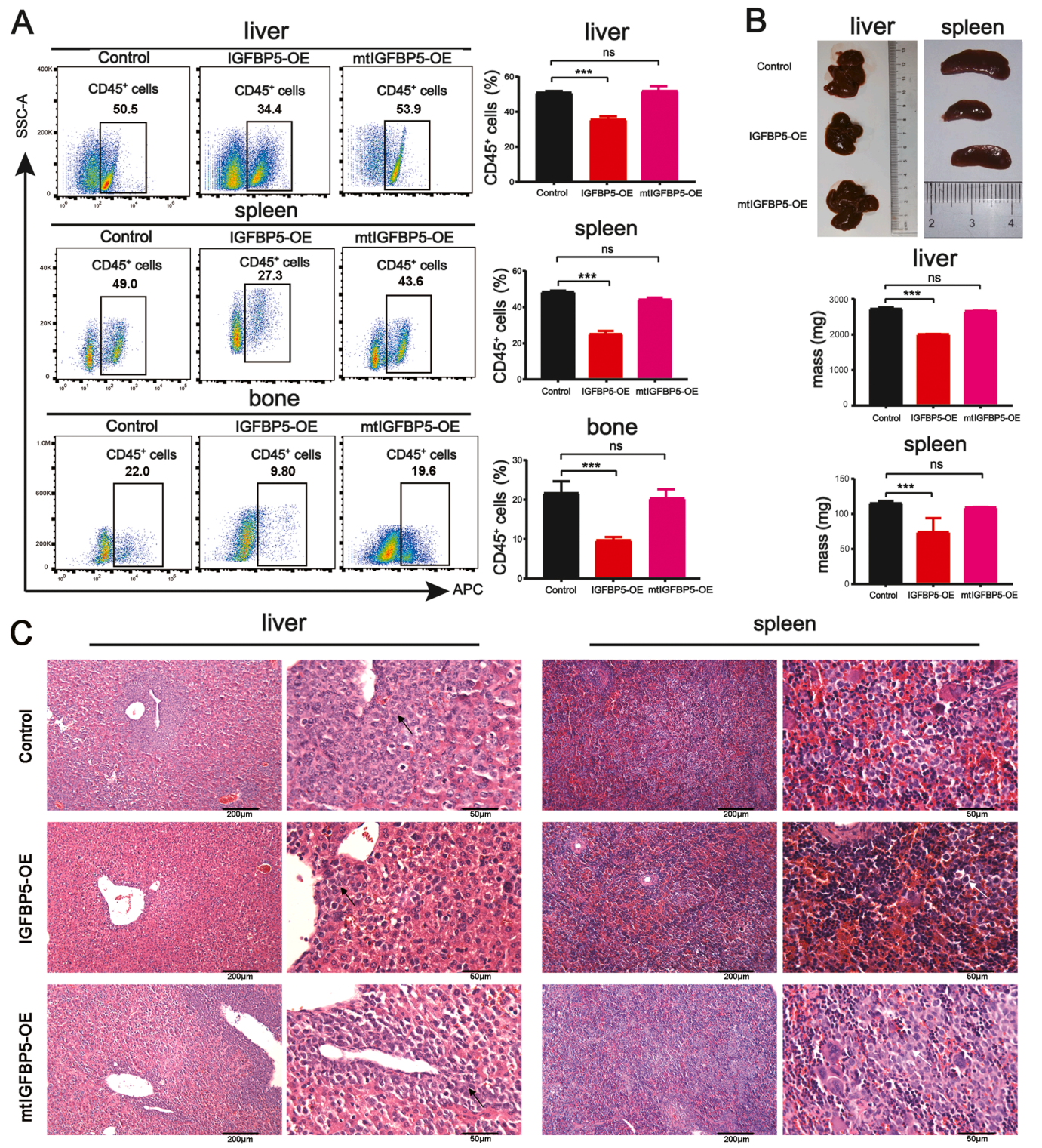

Fig. 6. Secreted IGFBP5 suppresses AML progression and extramedullary invasion in xenografts.
(A) Representative flow cytometry data showing the proportions of engrafted cells in bone marrow, liver, and spleen from NCG mice using an APC-labeled antibody to human CD45. U937 cells (4.0×10^5 cells per mouse) were transplanted into NCG mice by tail vein injection. After euthanizing the mice, the femurs, livers, and spleens were preserved for analysis. The quantification is shown on the right. (B) Image of the liver and spleen of the recipient mice at one month after transplantation. (C) Representative micrographs of hematoxylin/eosin staining for AML cell infiltration in the livers and spleens of mice transplanted with U937 cells carrying empty vector, IGFBP5 or mtIGFBP5. Liver showing less perivascular infiltration (arrows) by leukemic cells in mice transplanted with U937 cells carrying IGFBP5. Spleen showing less effacement of normal spleen architecture in mice transplanted with U937 cells carrying IGFBP5. Control: the mice transplanted with U937 cells carrying empty vector; IGFBP5-OE: the mice transplanted with U937 cells carrying IGFBP5. mtIGFBP5-OE: the mice transplanted with U937 cells carrying mtIGFBP5. The infiltrated leukemic cells are indicated by arrows (black arrows for liver, white arrows for spleen). Statistical significance was determined by ANOVA with Tukey's multiple comparison test. * $P < 0.05$; ** $P < 0.01$; *** $P < 0.001$; ns, not significant.

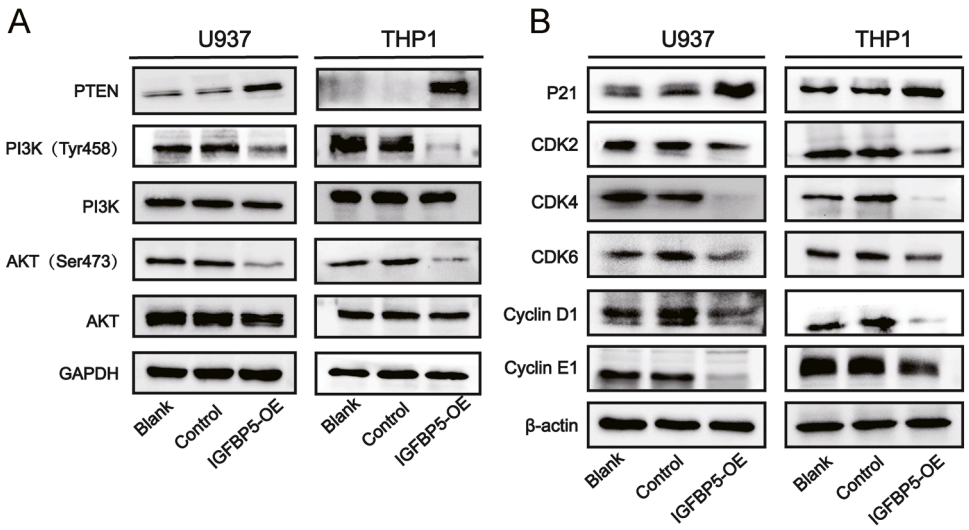

Fig. 7. Secreted IGFBP5 inhibits IGF1R-mediated PI3K/AKT pathway.
(A) Immunoblotting of PI3K/AKT signaling pathway molecules in IGFBP5-transduced THP1 and U937 cells. GAPDH was used as a loading control. (B) Immunoblotting of some cell cycle-related proteins in IGFBP5-transduced THP1 and U937 cells. β-actin was used as a loading control. Blank: the untreated parental cells; Control: the empty vector-transduced cells; IGFBP5-OE: the IGFBP5-transduced cells.

survival in the patients with lung cancer [19]. The data from three independent databases demonstrated that the AML patients with high IGFBP5 expression had a better OS compared with those with low IGFBP5 expression, suggesting that IGFBP5 may be considered as a good prognostic marker and function as a tumor suppressor in AML and up-regulation of IGFBP5 might delay AML progression. In contrast, high levels of serum IGFBP1, IGFBP2, and IGFBP6 were related with worse OS and poor progression-free survival of the AML patients [20]. This discrepancy may be attributed to the cellular context-dependent functions of IGFBPs.

Depending on the tumor type, IGFBP5 has either inhibitory or stimulatory effects on tumorigenesis [21]. IGFBP5 suppressed tumor growth and metastasis in ovarian cancer [22] and gastric cancer [23] and enhances radiosensitivity in prostate cancer [24]. On the contrary, IGFBP5 may contribute to cell proliferation of papillary thyroid carcinoma [25] and facilitate prostate cancer metastasis [26]. Here, our results demonstrated that the ectopical expression of IGFBP5 or addition of extrinsic rhIGFBP5 inhibited AML cell growth by inducing cell apoptosis and arresting G1/S transition and sensitized AML cells by enhancing DNR and Ara-C-induced cell apoptosis, suggesting that AML patients may benefit from a combination therapy consisting of IGFBP5 and chemotherapy.

It has been reported that exogenous and endogenous IGFBPs may exert different functions on cells [27]. IGFBP5 has different biological functions depending on its subcellular localization in host cells. With translocation of IGFBP5 protein from cytoplasm to nucleus, its function can be switched from a growth and migration stimulation to a growth inhibition in breast cancer [28]. To determine whether secreted or intracellular IGFBP5 inhibited AML cell growth, we generated an expression construct containing a mtIGFBP5 which deleted secretory signal peptide. Deletion of the native secretory signal peptide often give rise to an inability of the protein to excrete [29]. Our ELISA results also support that the ectopically expressed IGFBP5 but not mtIGFBP5 could be secreted into the culture supernatant. Ectopic expression assays of mtIGFBP5 and rhIGFBP5 protein stimulation assays verified that secreted rather than intracellular IGFBP5 served as a suppressor and chemosensitizer of AML cells. Xenograft model also showed that secreted rather than intracellular IGFBP5 delayed AML progression and extramedullary invasion *in vivo*. Conversely, our previous study reveals that intracellular rather than secreted IGFBP2 supports survival and migration of AML cells [30]. The underlying mechanisms for this discrepancy remain unknown and need to be further investigated.

IGFBP5 are involved in regulation of many pathways, including but not limited to AKT, extracellular-signal-regulated kinases, nuclear factor kappa-B, vascular endothelial growth factor, and transforming growth factor-β, each of which induces a distinct cancer phenotype [31]. IGFBP5 are implicated in tumorigenesis in IGF-dependent and -independent manner. The IGF1/IGF1R axis plays a critical role in various cancers, including AML, the activation of which can induce tumor cell proliferation, survival and chemoresistance [32]. Phospho-IGF1R (activated) rather than total IGF1R is an indicator of poor prognosis for cancers [33]. IGFBP5 can bind to circulating IGFs with high affinity [34]. IGFBP5 also can block IGF1 signaling by binding to IGF1 and sequestering its interaction with IGF1R [7]. On the other hand, IGFBP5 could potentiate the function of IGF1 by better presenting IGF1 to IGF1R [35]. AML cells can secrete IGF1 to support self-renewal and proliferation [13]. In our study, we found that extracellular rather than intracellular IGFBP5 inhibits IGF1R activity. Like other receptor tyrosine kinases, IGF1R phosphorylation can activate PI3K/AKT signaling pathway [36,37]. It had been reported that IGF1R/PI3K/AKT/mTOR (Mammalian target of rapamycin) pathway was critical to biological functions of AML cells, (such as growth, proliferation, migration), the blockade of which would suppress leukemia initiation and propagation [13]. Therefore, we propose that secreted IGFBP5 suppresses AML progression and metastasis through deactivating IGF1R-mediated PI3K/AKT pathway. Our study exactly confirmed that the phosphorylation of PI3K, AKT and IGF1R were attenuated in the cells that stably and ectopically expressed IGFBP5. PI3K/AKT pathway is involved in IGF1R-mediated apoptosis prevention and cell cycle distribution in hematopoietic cells [38]. Another study also confirmed that the deactivation of the IGF1R-mediated PI3K/AKT pathway with formononetin resulted in cell cycle arrest at G1/S transition in breast cancer cells [39]. Similarly, our study indicated that secreted IGFBP5 delayed G1/S phase transition of AML cells by dysregulating some critical cell cycle-related protein *via* IGF1R-mediated PI3K/AKT pathway.

Conclusion

In sum, our current study demonstrated that secreted rather than intracellular IGFBP5 inhibited AML cells growth and enhanced chemosensitivity of AML cells to DNR and Ara-C by inducing cell apoptosis and blocking G1/S phase transition *in vitro*. Accordingly, secreted rather

than intracellular IGFBP5 suppressed AML progression and extramedullary invasion in an *in vivo* xenograft model. Secreted IGFBP5 exerts its effects via blocking IGF1R-mediated PI3K/AKT pathway. Secreted IGFBP5 might be qualified as a useful therapeutic target against AML and enhancing IGFBP5, by overexpression or addition of rhIGFBP5, may be a suitable therapeutic and/or preventive approach for AML.

Availability of data and materials

The data and materials that support the findings here are available from the corresponding authors upon reasonable request.

CRediT authorship contribution statement

Beiying Zhang: Methodology, Validation, Formal analysis, Investigation, Data curation. **Xiaoling Deng:** Methodology, Visualization, Investigation. **Ruolan You:** Methodology, Investigation. **Jingru Liu:** Methodology, Investigation. **Diyu Hou:** Methodology, Investigation. **Xiaoting Wang:** Methodology, Investigation. **Shucheng Chen:** Methodology, Investigation. **Dongliang Li:** Methodology, Supervision. **Qiang Fu:** Methodology. **Jingdong Zhang:** Methodology, Validation. **Huifang Huang:** Conceptualization, Project administration, Funding acquisition, Supervision. **Xiaoli Chen:** Conceptualization, Project administration, Funding acquisition, Supervision, Writing – original draft, Writing – review & editing.

Declaration of Competing Interest

The authors declare no competing interests exist.

Fundings

This project was supported by grant from the National Natural Science Foundation of China (81760034, 81960035), the Natural Science Foundation of Jiangxi Province (20161BAB205202, 20192ACBL20006), Jiangxi Province Health Commission Topic (202310097), the government-funded project of the construction of high-level laboratory (Min201704), National Key Clinical Specialty Discipline Construction Program (2021-76) and Fujian Provincial Clinical Research Center for Hematological Malignancies (2020Y2006).

References

[1] M. Spreafico, A. Gruszka, D. Valli, M. Mazzola, G. Deflorian, A. Quintè, M. Totaro, C. Battaglia, M. Alcalay, A. Marozzi, et al., HDAC8: a promising therapeutic target for acute myeloid leukemia, Front. Cell Dev. Biol. 8 (2020) 844.
[2] R. Siegel, K. Miller, A. Jemal, Cancer statistics, 2020, CA Cancer J. Clin. 70 (2020) 7–30.
[3] K. Siveen, S. Uddin, R. Mohammad, Targeting acute myeloid leukemia stem cell signaling by natural products, Mol. Cancer 16 (2017) 13.
[4] S. Díaz Del Moral, M. Benaouicha, R. Muñoz-Chápuli, R. Carmona, The insulin-like growth factor signalling pathway in cardiac development and regeneration, Int. J. Mol. Sci. 23 (1) (2021) 234, https://doi.org/10.3390/ijms23010234.
[5] B. Altieri, A. Colao, A. Faggiano, The role of insulin-like growth factor system in the adrenocortical tumors, Minerva Endocrinol. 44 (2019) 43–57.
[6] G. Güllü, S. Karabulut, M. Akkiprik, Functional roles and clinical values of insulin-like growth factor-binding protein-5 in different types of cancers, Chin. J. Cancer 31 (2012) 266–280.
[7] D. Salih, G. Tripathi, C. Holding, T. Szestak, M. Gonzalez, E. Carter, L. Cobb, J. Eisemann, J. Pell, Insulin-like growth factor-binding protein 5 (Igfbp5) compromises survival, growth, muscle development, and fertility in mice, Proc. Natl. Acad. Sci. USA 101 (2004) 4314–4319.
[8] L. Bach, IGF-binding proteins, J. Mol. Endocrinol. 61 (2018) T11–T28.
[9] X. Li, X. Cao, X. Li, W. Zhang, Y. Feng, Expression level of insulin-like growth factor binding protein 5 mRNA is a prognostic factor for breast cancer, Cancer Sci. 98 (2007) 1592–1596.
[10] L. Schedlich, S. Le Page, S. Firth, L. Briggs, D. Jans, R. Baxter, Nuclear import of insulin-like growth factor-binding protein-3 and -5 is mediated by the importin beta subunit, J. Biol. Chem. 275 (2000) 23462–23470.
[11] R. Baxter, IGF binding proteins in cancer: mechanistic and clinical insights, Nat. Rev. Cancer 14 (2014) 329–341.
[12] C. McCaig, C. Perks, J. Holly, Signalling pathways involved in the direct effects of IGFBP-5 on breast epithelial cell attachment and survival, J. Cell. Biochem. 84 (2002) 784–794.
[13] K. Doepfner, O. Spertini, A. Arcaro, Autocrine insulin-like growth factor-I signaling promotes growth and survival of human acute myeloid leukemia cells via the phosphoinositide 3-kinase/Akt pathway, Leukemia 21 (2007) 1921–1930.
[14] Y. He, J. Zhang, J. Zheng, W. Du, H. Xiao, W. Liu, X. Li, X. Chen, L. Yang, S. Huang, The insulin-like growth factor-1 receptor kinase inhibitor, NVP-ADW742, suppresses survival and resistance to chemotherapy in acute myeloid leukemia cells, Oncol. Res. 19 (2010) 35–43.
[15] J. Dittmer, Biological effects and regulation of IGFBP5 in breast cancer, Front. Endocrinol. 13 (2022), 983793.
[16] P. Liang, Y. Wang, T. Wu, W. Wu, A. Liao, K. Shen, C. Hsing, Y. Shiue, H. Huang, H. Hsu, et al., IGFBP-5 overexpression as a poor prognostic factor in patients with urothelial carcinomas of upper urinary tracts and urinary bladder, J. Clin. Pathol. 66 (2013) 573–582.
[17] S. Wang, Q. Hong, X. Geng, K. Chi, G. Cai, D. Wu, Insulin-like growth factor binding protein 5-a probable target of kidney renal papillary renal cell carcinoma, Biomed. Res. Int. 2019 (2019), 3210324.
[18] Y. Deng, X. Yang, H. Hua, C. Zhang, IGFBP5 is upregulated and associated with poor prognosis in colorectal cancer, Int. J. Gen. Med. 15 (2022) 6485–6497.
[19] D. Shersher, M. Vercillo, C. Fhied, S. Basu, O. Rouhi, B. Mahon, J. Coon, W. Warren, L. Faber, E. Hong, et al., Biomarkers of the insulin-like growth factor pathway predict progression and outcome in lung cancer, Ann. Thorac. Surg. 92 (2011) 1805–1811, discussion 1811.
[20] R. Karmali, M. Larson, J. Shammo, S. Basu, K. Christopherson, J. Borgia, P. Venugopal, Impact of insulin-like growth factor 1 and insulin-like growth factor binding proteins on outcomes in acute myeloid leukemia, Leuk. Lymphoma 56 (2015) 3135–3142.
[21] Y. Su, E. Wagner, Q. Luo, J. Huang, L. Chen, B. He, G. Zuo, Q. Shi, B. Zhang, G. Zhu, et al., Insulin-like growth factor binding protein 5 suppresses tumor growth and metastasis of human osteosarcoma, Oncogene 30 (2011) 3907–3917.
[22] S. Rho, S. Dong, S. Kang, S. Seo, C. Yoo, D. Lee, J. Woo, S. Park, Insulin-like growth factor-binding protein-5 (IGFBP-5) acts as a tumor suppressor by inhibiting angiogenesis, Carcinogenesis 29 (2008) 2106–2111.
[23] L. Zhang, W. Li, L. Cao, J. Xu, Y. Qian, H. Chen, Y. Zhang, W. Kang, H. Gou, C. Wong, et al., PKNOX2 suppresses gastric cancer through the transcriptional activation of IGFBP5 and p53, Oncogene 38 (2019) 4590–4604.
[24] X. Chen, Q. Yu, H. Pan, P. Li, X. Wang, S. Fu, Overexpression of IGFBP5 enhances radiosensitivity through PI3K-AKT pathway in prostate cancer, Cancer Manag. Res. 12 (2020) 5409–5418.
[25] L. Liu, J. Wang, X. Li, J. Ma, C. Shi, H. Zhu, Q. Xi, J. Zhang, X. Zhao, M. Gu, MiR-204-5p suppresses cell proliferation by inhibiting IGFBP5 in papillary thyroid carcinoma, Biochem. Biophys. Res. Commun. 457 (2015) 621–626.
[26] C. Xu, L. Graf, L. Fazli, I. Coleman, D. Mauldin, D. Li, P. Nelson, M. Gleave, S. Plymate, M. Cox, et al., Regulation of global gene expression in the bone marrow microenvironment by androgen: androgen ablation increases insulin-like growth factor binding protein-5 expression, Prostate 67 (2007) 1621–1629.
[27] J. Pilewski, L. Liu, A. Henry, A. Knauer, C. Feghali-Bostwick, Insulin-like growth factor binding proteins 3 and 5 are overexpressed in idiopathic pulmonary fibrosis and contribute to extracellular matrix deposition, Am. J. Pathol. 166 (2005) 399–407.
[28] M. Akkiprik, L. Hu, A. Sahin, X. Hao, W. Zhang, The subcellular localization of IGFBP5 affects its cell growth and migration functions in breast cancer, BMC Cancer 9 (2009) 103.
[29] F. Birzele, G. Csaba, R. Zimmer, Alternative splicing and protein structure evolution, Nucleic Acids Res. 36 (2008) 550–558.
[30] X. Chen, J. Zheng, Y. Zou, C. Song, X. Hu, C. Zhang, IGF binding protein 2 is a cell-autonomousfactor supporting survival and migration of acute leukemia cells, J. Hematol. Oncol. 6 (2013) 72.
[31] J. Waters, I. Urbano, M. Robinson, C. House, Insulin-like growth factor binding protein 5: diverse roles in cancer, Front. Oncol. 12 (2022), 1052457.
[32] M. Pollak, The insulin and insulin-like growth factor receptor family in neoplasia: an update, Nat. Rev. Cancer 12 (2012) 159–169.
[33] J. Law, G. Habibi, K. Hu, H. Masoudi, M. Wang, A. Stratford, E. Park, J. Gee, P. Finlay, H. Jones, et al., Phosphorylated insulin-like growth factor-i/insulin receptor is present in all breast cancer subtypes and is related to poor survival, Cancer Res. 68 (2008) 10238–10246.
[34] V. Hwa, Y. Oh, R. Rosenfeld, The insulin-like growth factor-binding protein (IGFBP) superfamily, Endocr. Rev. 20 (1999) 761–787.
[35] H. Miyake, M. Pollak, M. Gleave, Castration-induced up-regulation of insulin-like growth factor binding protein-5 potentiates insulin-like growth factor-I activity and accelerates progression to androgen independence in prostate cancer models, Cancer Res. 60 (2000) 3058–3064.
[36] A. Gaben, M. Sabbah, G. Redeuilh, M. Bedin, J. Mester, Ligand-free estrogen receptor activity complements IGF1R to induce the proliferation of the MCF-7 breast cancer cells, BMC Cancer 12 (2012) 291.
[37] S. Johnson, R. Haun, Insulin-like growth factor binding protein-5 influences pancreatic cancer cell growth, World J. Gastroenterol. 15 (2009) 3355–3366.
[38] M. Wu, Y. Tang, G. Hu, C. Yang, K. Ye, X. Liu, miR-4458 directly targets IGF1R to inhibit cell proliferation and promote apoptosis in hemangioma, Exp. Ther. Med. 19 (2020) 3017–3023.
[39] J. Chen, J. Zeng, M. Xin, W. Huang, X. Chen, Formononetin induces cell cycle arrest of human breast cancer cells via IGF1/PI3K/Akt pathways *in vitro* and *in vivo*, Horm. Metab. Res. = Horm. Stoffwechselforsch. = Horm. Metab. 43 (2011) 681–686.